The 14th World Conference on Earthquake Engineering
October 12-17, 2008, Beijing, China

# Elasto-plastic Effective Stress Analysis of Centrifugal Shaking Tests of a Rockfill Dam

**T. Iwashita**

*Deputy Team Leader, Hydraulic Engineering Group, Public Works Research Institute, Tsukuba, Japan*
*Email: iwashita@pwri.go.jp*

**ABSTRACT:**

No earthquake has caused failure or severe damage to any rockfill dams with bodies of well-compacted rock materials. It is important to estimate the damage grade quantitatively in order to evaluate a seismic performance of a dam against a large earthquake. A centrifugal shaking model test of a rockfill dam was performed under centrifugal force field of 50g to investigate the seismic damage patterns of rockfill dams. The shake-induced deformation from sinusoidal wave shaking was limited to the high elevation rock zone near the slope top and the upper core. This shaking model test did not cause any deep failure surfaces. The dam behavior caused by the shaking test was simulated by the elasto-plastic effective stress analysis incorporating a constitutive equation which can simulate the cyclic mobility of compacted rock materials. The analysis succeeded in reproducing most of the state of deformation in the core and high elevation zone of the upstream rock. The elasto-plastic effective stress FE analysis seems to be a useful prediction method for use as an analytical method to predict earthquake-induced displacement of rockfill dams.

**KEYWORDS:** rockfill dam, effective stress analysis, elastoplasticity, constitutive equation, centrifugal shaking test

## 1. INTRODUCTION

The cross section of rockfill dams in Japan is designed based on slope stability, which means no damage by sliding of the dam body for lateral seismic force (as scale of usual earthquake motions). To perform seismic design for a Level 2 earthquake, which is equivalent to the maximum credible earthquake, an evaluation is done to verify whether or not the earthquake-induced residual deformation estimated by numerical analysis is below the allowed displacement. No earthquake has caused failure or severe damage to any well-constructed rockfill dams, leaving many unclear facts concerning the patterns of ultimate failure and of damage to a rockfill dam caused by an extremely large earthquake. It is, therefore, important to perform shaking testing of a model of a rockfill dam as testing to verify patterns of failure and damage. A centrifugal shaking model test is an effective method to study the behavior of massive structures such as dams during earthquakes, but few centrifugal tests for a rockfill dam have been performed.

Earthquake-induced residual deformation is generally estimated by calculation based on the Newmark sliding block analysis: hypothesizing the potential failure surface then calculating the earthquake-induced displacement of the sliding mass assumed to be rigid. With this method, however, the damage pattern is assumed to be only sliding failure of the dam body even in the case of a rockfill dam made of mainly rock materials with large grain sizes. The response analysis is performed using the equivalent linear method, so it cannot accurately reproduce non-linearity accompanying large deformation. Dynamic elasto-plastic FE analysis would eliminate these problems. Effective stress analysis which deals with problems such as liquefaction for loose sand has been performed applying a variety of constitutive models. It is, however, rare for effective stress analysis to be applied with well-compacted rock materials, such as that of a rockfill dam with cyclic mobility behavior.

This paper first describes large-scale centrifugal shaking table tests performed using the model of a rockfill dam with a central clay core. Next, a numerical simulation of deformation behavior by the model test was performed using elasto-plastic effective stress analysis. In this analysis, the constitutive equation of soils was able to simulate cyclic mobility behavior.

## 2. CENTRIFUGAL SHAKING MODEL TEST

### *2.1. Testing Method*

Large centrifugal shaking tests of models of a rockfill dam with a central clay core were carried out. The dam model was 40cm high, 150cm long and 30cm wide. Its upstream slope gradient was 1:2.0 and its downstream slope gradient was 1:1.7. The model was made of dam materials from the actual rockfill dam. The rock materials were stabilized with grading identical to that of the actual dam, and their maximum grain size was adjusted to 9.75mm. The properties of the dam model materials are shown in Table 1. The dam model started to be made by forming only the core which was compacted with each layer of a thickness of 15mm. After the core was completed, a centrifugal force of 50g was loaded to adequately consolidate the core model. Next rock materials were placed at a thickness of 20mm per layer and compacted to a D-value of 108 using a vibrator. The water level was set at 90% of the dam height assuming the full water level. The testing was carried out at a centrifugal force field of 50g. Sinusoidal waves of 50Hz and 20 cycles were input to the shaking table. Their acceleration amplitude increased in six steps from 5g (98gal at gravitational force field) to 30g (588 gal at gravitational force field).

Table1 Properties of dam model materials

| | Core material | Rock material | |
|---|---|---|---|
| | | Upstream side | Downstream side |
| Dry Density (g / cm$^3$) | 1.68 | 2.25 | 2.24 |
| Water Content (%) | 11.4 | 4.9 | |
| D-value (%) | 94.5 | 108.7 | 108.3 |
| Maximum Grain Size (mm) | 4.75 | 9.75 | |
| Mean Grain Size (mm) | 0.5 | 3.0 | |
| Uniformity Coefficient | | 12 | |
| S-wave Velocity (m/s) | 490 | 550 | 460 |
| Permeability Coefficient (cm/s) | | $1.59\times10^{-2}$ | |

### *2.2. Test Results*

Photograph 1 shows original dam model before shaking and the state of the model after final shaking at Step 6. Figure 1 shows the comparison between the original configuration and final configuration after Step 6, and Figure 2 shows the displacement vectors in the dam body. Figure 4 shows the cumulative settlement of the crest at each shaking step.

Original model

Final model
after Step 6

Photo.1 Original model before shaking and final model after shaking Step 6 for centrifugal test

As Figure 3 shows, until shaking Step 3 (input acceleration of 294 gal at gravitational force field), almost no deformation occurred, and large deformation of the dam model began from Step 4. At Step 4, rocks near the top of the upstream side slope slipped slightly, so the top of the core leaned slightly towards the upstream side. At the same time, rocks from the top of the downstream slope felt down slightly. At Step 5, deformation expanded as it did at Step 4. Step 6 shaking caused the rock at the top of both the upstream and downstream slopes to completely fail and the exposed core top to lean largely towards the upstream side. The part of the dam that was extremely deformed was limited to that close to the top of the upstream side. The deep parts of the dam or low elevation parts were hardly deformed.

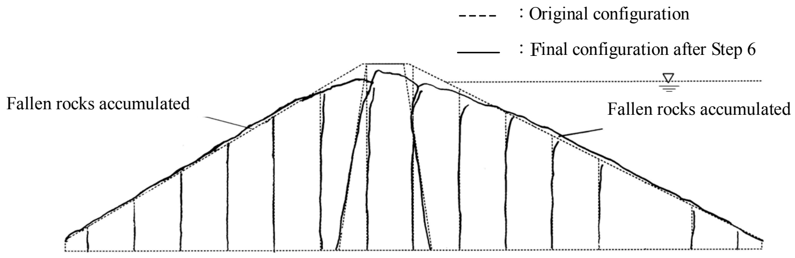


Fig.1 Residual deformation of centrifugal model after shaking Step 6

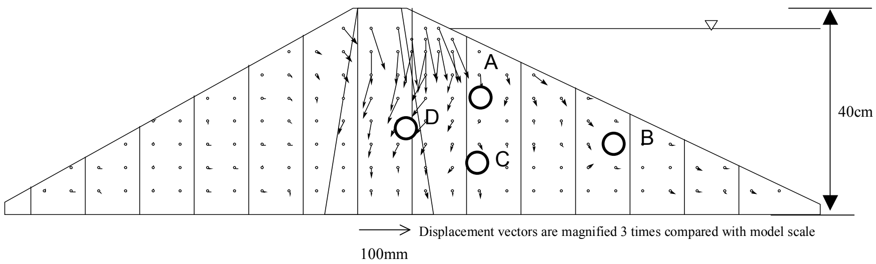


Fig.2 Displacement vectors in the model after shaking Step 6

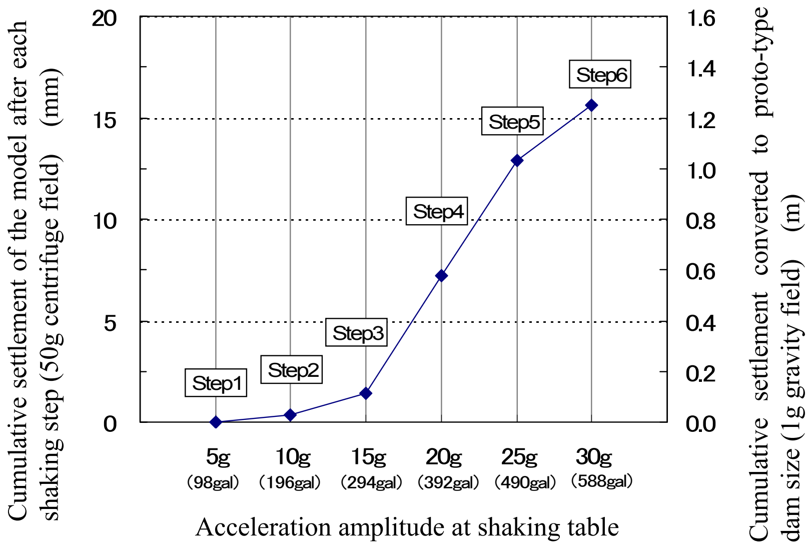


Fig.3 Cumulative settlement of crest after each shaking step

The rocks on the top of the upstream slope failed severely from the upstream side, so the top of the core largely leaned upstream as it settled. Slight deformation, which was limited to the shallow layer of the upstream slope submerged at the medium elevations, occurred along the slope, but bulging did not occurred. Figure 1 shows that although the upstream and downstream slopes seem to bulge slightly, this was the accumulation of rocks which fell down from near the tops of the slopes. No failure surface capable of forming a deep slide appeared.

Figures 4 and 5 show the time history of the excess pore water pressure ratio and acceleration inside of the dam model at Step 5. Four measurement Points A to D are shown in the figures: the high elevation and slope shallow layer of the rock zone which was largely deformed (Point A), medium elevation of the slope shallow layer which was hardly deformed (Point B), central zone of rock (Point C) and inside of the core (Point D). Despite the strong shaking of 490gal at gravitational force field, the residual excess pore water pressure ratio was extremely low. This finding is quite different from the result obtained from the similar centrifugal shaking table test of an earth dam (Iwashita *et al,* 2001): residual excess pore water pressure ratio up to 1.0 in the shallow layer of the slope of an earth dam resulted in large deformation. The dissipation of the excess pore water pressure in the rock zone is much faster than that seen in results for earth dam tests. The mechanism that deformed the upper rock zone of the rockfill dam model is probably not based only on the increase of the excess pore water pressure. In the rock zone, large negative pore water pressure was produced, and the acceleration time histories at Points A and B in the shallow layer, unlike that of Point C in the center of the dam model, are sharply pointed wave forms. That shows the behavior of cyclic mobility of rock materials.

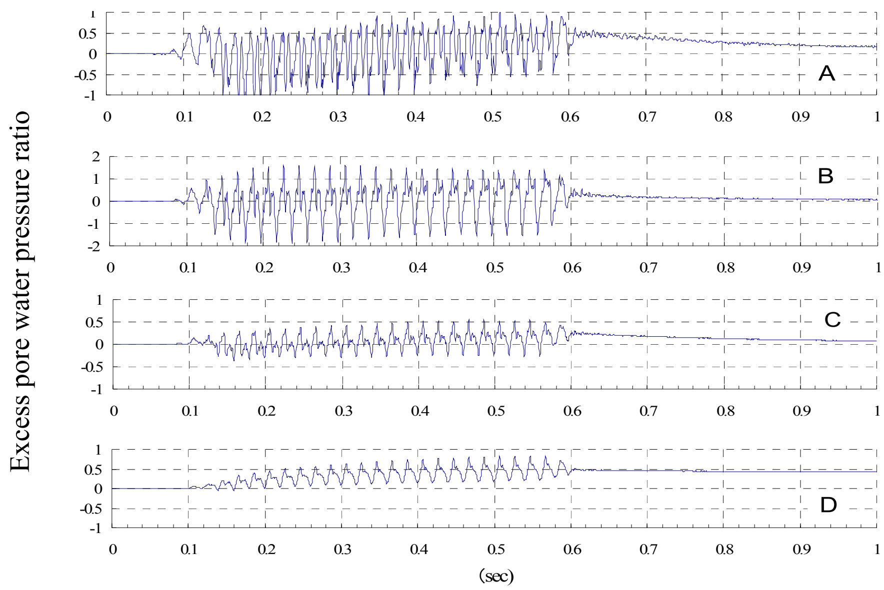


Fig.4 Time histories of excess pore water pressure ratio in the model during shaking Step 5

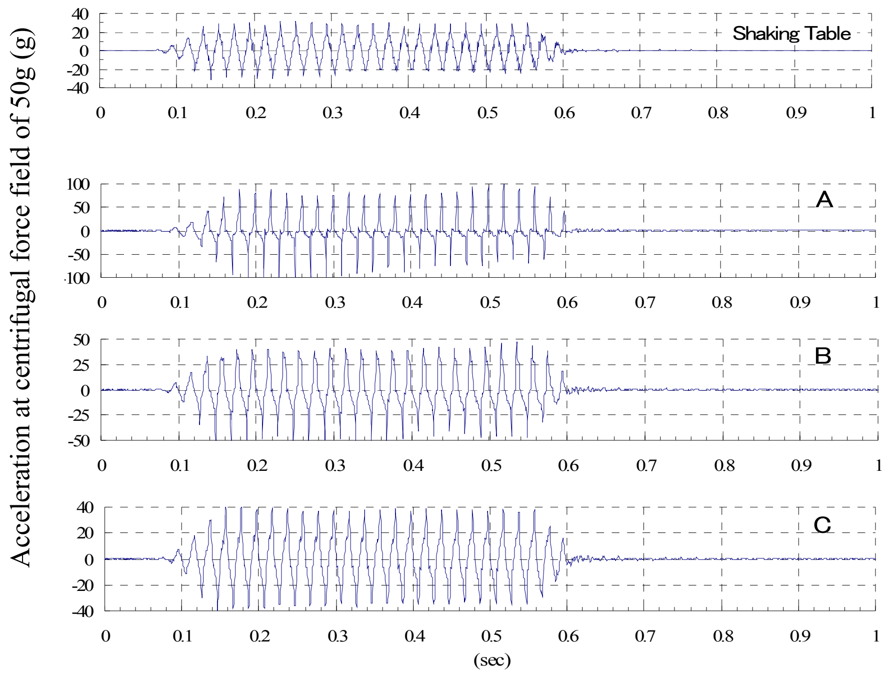


Fig.5 Time histories of response acceleration in the model during shaking Step 5

## 3. SIMULATION BY ELASTO-PLASTIC EFFECTIVE STRESS ANALYSIS

### *3.1. Analysis Method*

The behavior of centrifugal shaking of the rockfill dam model was simulated using dynamic elasto-plastic effective stress analysis. The FE model of the dam model in the centrifugal shaking tests was prepared based on the results of laboratory material tests. The submerged part of the dam body was modeled by two phase formulations of soil (solid) and water (fluid) and the other part was modeled by one phase formulation of soil only. The internal friction angle that defines the failure line in the submerged part of the rock zone was set based on drained monotonic loading torsional shear tests. The rock zone of one phase formulation was modeled based on Mohr-Coulomb's yield rule using the results of drained triaxial compressive tests.

The program code MuDIAN (Shiomi *et al,* 1998) was used to perform effective stress analysis. Shaking Step 4 when conspicuous deformation began on the centrifugal shaking tests was analyzed for simulation. The shaking acceleration amplitude is 392gal at gravitational force field. Horizontal and vertical components of the acceleration observed at the bottom of the dam model were input to the FE model.

### *3.2. Constitutive Equation of Dam Materials*

To accurately represent the dynamic strength properties of well-compacted rock materials, the submerged rock materials were modeled by the modified Densification model which is based on the Densification model (Zienkiewicz *et al*, 1978). The characteristic of the Densification model is that considering the hardening law for volumetric strain $\varepsilon_v^p$ due to the dilatancy and the hardening law for shear strain $\varepsilon_s^p$ independently, that is, plastic strain in incremental form is able to express as the following: $d\varepsilon^p = d\varepsilon_v^p + d\varepsilon_s^p$. The parameters of the constitutive equation of soils can, therefore, be directly obtained from the results of soil tests. In the modified Densification model, only the autogeneous volumetric strain increment $d\varepsilon_{vo}$ produced by dilatancy is considered as the plastic volumetric strain increment $d\varepsilon_v^p$ (Zienkiewicz *et al*, 1999). This model can simulate cyclic mobility after the stress point reaches the phase transformation line, which is the most important factor in simulating the dynamic behavior of dense soils and rocks such as rockfill dam.

The plastic shear strain increment $d\varepsilon_s^p$ is calculated incorporating the concept of the subloading surface model (Hashiguchi *et al*, 1996). The subloading surface model can consider the production of plastic strain, even inside the yield surface. The plastic shear strain increment $d\varepsilon_s^p$ was calculated by treating Mohr-Coulomb's yield surface, which is based on the non-associated flow rule with plastic volumetric strain of zero, as the subloading surface.

The parameters of the modified Densification model were set from the element test results based upon undrained cyclic loading torsional shear testing using a cylindrical specimen with an external diameter of 800mm, an internal diameter of 400mm and a height of 800mm. The grain size distribution curve of the rock materials of the specimens was set to parallel to that of the rock materials used to make the dam model for the centrifugal test. Figures 6 and 7 show the comparison of cyclic shear strength and effective stress paths from laboratory tests and computed analytical simulations using the modified Densification model respectively. Element analysis agrees closely with the laboratory test and expresses the cyclic mobility.

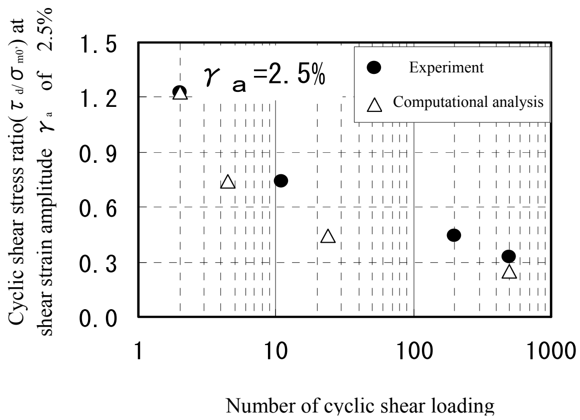


Fig.6 Comparison of cyclic shear strength between element experiment and its analysis

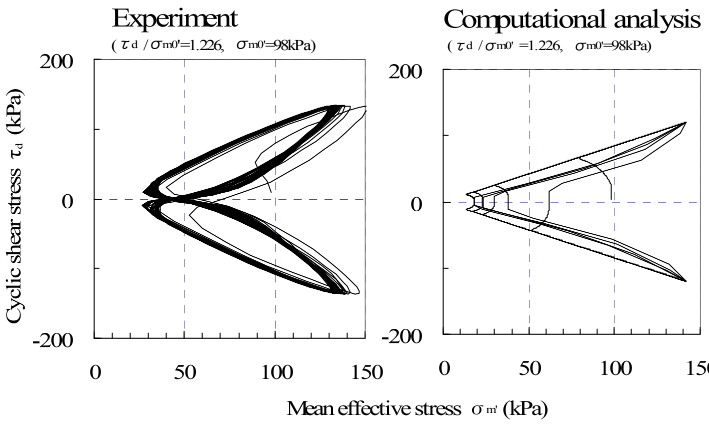


Fig.7 Comparison of effective stress paths between element experiment and its analysis

### *3.3. Analysis Results*

Figure 8 shows the displacement vectors superimposed on the final configuration obtained by simulation analysis of Step 4. Comparing it with the configuration of deformation after Step 6 of the shaking model test shown in Figure 2 has revealed the following facts. **a)** Results of the model test and analysis both showed large deformation of the high elevation rock zone of the upstream side. However, the analysis indicated the occurrence of bulging near the upstream toe. This was almost never seen in the results of model tests. **b)** Both the test and analysis showed deformation of the top of the core causing it to lean towards the upstream side. **c)** The almost complete absence of deformation of the downstream rock zone is identical to the results of the model tests. **d)** The settlement of the high elevation part of the submerged part on the upstream side was shown by both the analysis and the test. On the high elevation part of the shallow layer of the upstream slope, the analysis revealed large residual displacement parallel to the slope, while the model test indicated little residual displacement. **e)** While the model test showed the largest residual deformation near the crest of upstream slope, the analysis results indicated that the occurrence of the largest displacement on the upstream slope was a little above an elevation that is about 1/2 of the dam height.

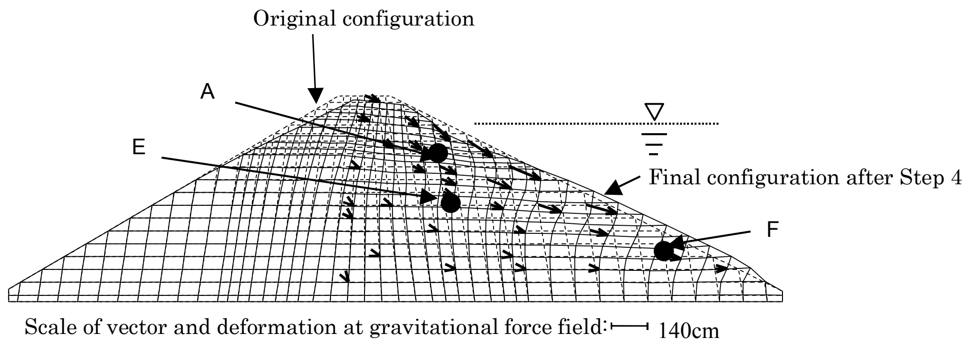


Fig.8 Residual deformation by simulation of shaking Step 4

Figure 9 compares the time histories of the settlement and horizontal displacement of the center of the dam crest according to the model test and the analysis. Final settlements of the test and analysis are in close agreement, while final horizontal displacement of the analysis is larger than the test. This seems to be a result of the fact that while the model test showed almost no deformation near the upstream toe, the analysis showed the occurrence of deformation along the upstream slope which included bulging.

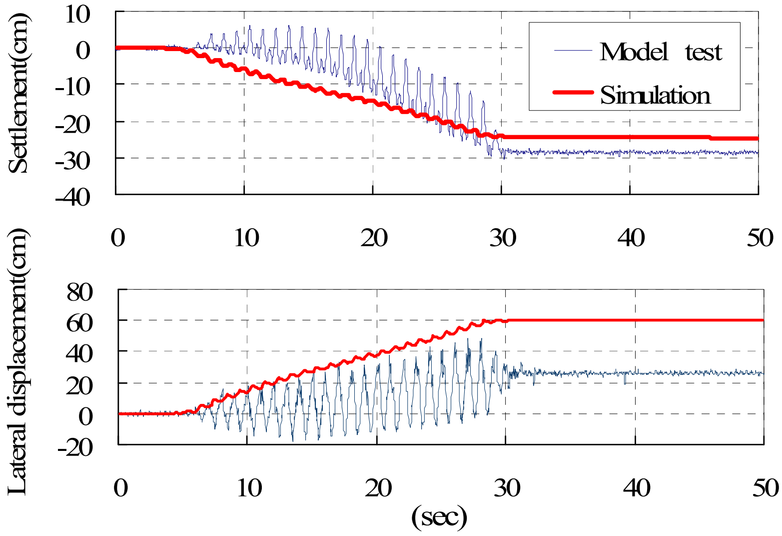


Fig.9 Settlement and lateral displacement at crest with scale in gravitational force field at Step 4

Figure 10 shows the time history of excess pore water pressure ratio at three Points A, E and F in the rock zone shown in Figure 8. The analysis results are similar to the test results in that the amplitude of the excess pore water pressure ratio during shaking at Point A which is close to the shallow layer is larger than it is at Point E in the deep zone. The analysis results accurately reproduce the residual excess pore water pressure ratio and the dissipation process of the excess pore water pressure in post-shaking from the model testing at the Points A and E. At Point F near the upstream toe, little excess pore water pressure ratio is generated in the model test, while for the analysis, large excess pore water pressure during shaking is generated and the residual excess pore water pressure is also high. The analysis result seems to indicate that generation of large excess pore water pressure near the toe slope caused a decrease in the strength of dam body due to the loss of the effective stress, and which consequently resulted in the bulging at the upstream slope.

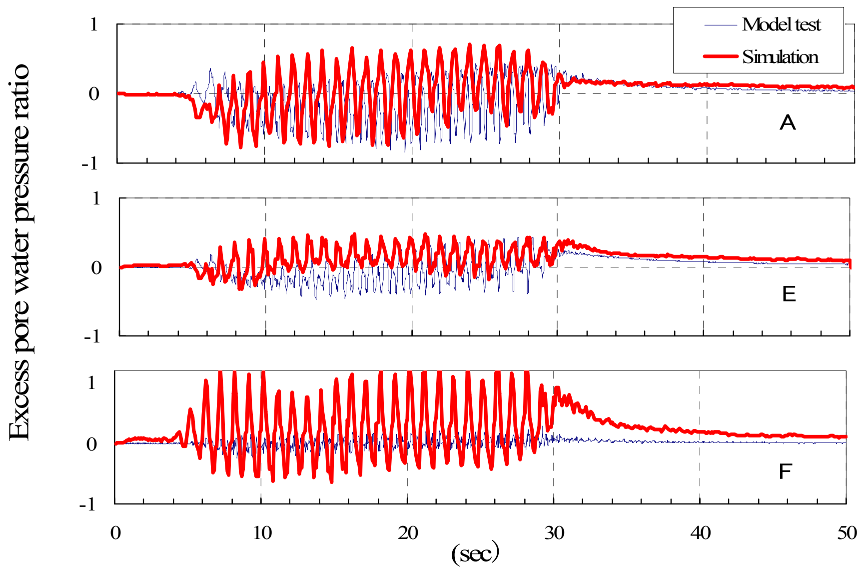


Fig.10 Time histories of excess pore water pressure ratio at Step 4

## 4. CONCLUSIONS

A centrifugal shaking model test of a rockfill dam was performed under centrifugal force field of 50g to investigate the seismic damage patterns of rockfill dams. The dam began shake-induced deformation from sinusoidal wave shaking of above 400gal at gravitational force field converted, but the deformed area was limited to the high elevation rock zone near the slope top and upper core. Even at shaking of 600gal, a deep failure surface did not occur.

The dam behavior by the model test was simulated by elasto-plastic effective stress analysis incorporating a constitutive equation which can simulate the cyclic mobility of compacted rock materials. The analysis succeeded in reproducing most of the state of deformation in the core and high elevation zone of the upstream rock, however bulging near the upstream toe which did not occur in the model tests appeared in the analysis results.

The centrifugal model tests revealed that the damage pattern of rockfill dams caused by earthquakes is not only sliding failure. As analytical methods to predict the earthquake-induced displacement of rockfill dams, elasto-plastic effective stress FE analysis, which is a combined constitutive equation model considering cyclic mobility of rock materials, seems to be useful.

## REFERENCES

Hashiguchi, K. *et al.* (1996). Elasto-plastic constitutive equation of soils based on the concepts of subloading surface and rotational hardening, *Journal of Japan Society of Civil Engineers* **No.547/Ⅲ-36**, 127-144. (in Japanese)

Iwashita, T. and Yamamoto, S. *et al.* (2001). Centrifuge model tests of an earth dam damaged due to the 1995 Kobe Earthquake, *Proceedings of the 36th Japan National Conference on Geotechnical Engineering,* Japanese Geotechnical Society, 1347-1348. (in Japanese)

Shiomi, T. *et al.* (1998). Development of structural analysis system considering nonlinearity of foundation and structure, *Report of Research & Development Institute, Takenaka Co.* **No.54**, 1-8. (in Japanese)

Zienkiewicz, O.C. *et al.* (1978). Nonlinear Seismic Response and Liquefaction, *Int. Journal of Numerical and Analytical Method in Geomechanics* **2(4)**, 381-404.

Zienkiewicz, O.C. *et al.* (1999). Computational geomechanics with special reference to earthquake engineering, John Wiley & Sons, West Sussex, U.K.